ACS APPLIED MATERIALS & INTERFACES

Research Article

www.acsami.org

Antifungal Activity and Mechanism of Palladium-Modified Nitrogen-Doped Titanium Oxide Photocatalyst on Agricultural Pathogenic Fungi *Fusarium graminearum*

Jingtao Zhang,[†] Yang Liu,[†] Qi Li,*[,†] Xiaoping Zhang,[‡] and Jian Ku Shang[†,§]

[†]Environment Functional Materials Division, Shenyang National Laboratory for Materials Science, Institute of Metal Research, Chinese Academy of Sciences, 72 Wenhua Road, Shenyang, Liaoning Province, 110016, P. R. China

[‡]Department of Microbiology, College of Resource and Environment, Sichuan Agricultural University, Chengdu, Sichuan province, 611130, P. R. China

[§]Department of Materials Science and Engineering, University of Illinois at Urbana-Champaign, Urbana, Illinois 61801, United States

ABSTRACT: *Fusarium graminearum* is the pathogen for *Fusarium* head blight (FHB) on wheat, which could significantly reduce grain quality/yield and produce a variety of mycotoxins posing a potential safety concern to human foods. As an environmentally friendly alternative to the commonly used chemical fugicides, a highly effective photocatalytic disinfection of *F. graminearum* macroconidia under visible light illumination was demonstrated on a visible-light-activated palladium-modified nitrogen-doped titanium oxide (TiON/PdO) nanoparticle photocatalyst. Because of the opposite surface charges of the TiON/PdO nanoparticles and the *F. graminearum* macroconidium, the nanoparticles were strongly adsorbed onto the macroconidium surface, which is beneficial to the photocatalytic disinfection of these macroconidia. The photocatalytic disinfection mechanism of TiON/PdO nanoparticles on these macroconidia could be attributed to their cell wall/membrane damage caused by the attack from reactive oxygen species (ROSs) as demonstrated by the fluorescence/phase contrast microscopy observations, while a breakage of their cell structure was not necessary for their loss of viability.

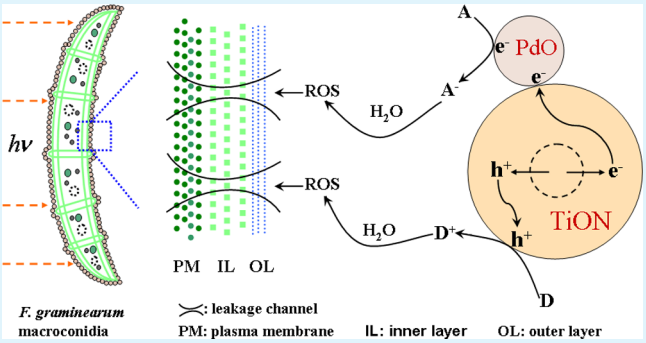

KEYWORDS: *Fusarium graminearum macroconidia, TiON/PdO nanoparticles, photocatalytic disinfection, visible light, fluorescence staining*

1. INTRODUCTION

As a common plant disease, *Fusarium* head blight (FHB) is one of the devastating diseases on small grain cereal crops,[1,2] which could significantly reduce grain quality and yield. FHB could also produce a variety of mycotoxins which are detrimental to livestock and pose a potential safety concern to human foods. *F. graminearum* (teleomorph *Gibberella zeae*) is the pathogen which causes FHB on wheat.[3] The macroconidia formed by *F. graminearum* plays an important role in the dissemination of FHB. The conventional fungicidal methods rely heavily on synthetic chemical pesticides. However, synthetic chemical pesticides are usually hazardous to animals and the environment due to their residual toxicity. Furthermore, fungi have developed resistance to some traditional fungicides, such as benzimidazoles and dicarboximides, which makes it more difficult to control fungal growth.[4] Thus, alternative antifungal approaches need to be developed, which should overcome the fungicide resistance for a better fungicidal effect while posing no harmful effect on the environment. It would be even better if it could also decompose mycotoxins produced by fungi.

In 1985, Matsunaga et al.[5] reported the first successful photocatalytic disinfection of microorganism by titanium dioxide (TiO_2). Since then, extensive research has been conducted on TiO_2-based photocatalysts for various microorganism disinfections, including viruses,[6] bacteria,[5,7,8] fungi,[5,9,10] bacterial/fungal spores,[11] algae,[12] and protozoa.[13] TiO_2 is considered as a leading candidate for potential photocatalytic applications because of its physical and chemical stability, relatively low cost, and high photocatalytic efficiency. It has been approved by the American Food and Drug Administration (FDA) for its use in human foods, drugs, cosmetics, and food contact materials in contact with unprotected foods.[14−16]

It is generally believed that the photocatalytic microorganism disinfection relies on the interaction between microorganisms and reactive oxygen species (ROSs) generated by photocatalysts upon their activation from proper light illumination

Received: August 1, 2013
Accepted: October 8, 2013
Published: October 8, 2013

that not only destroys microorganisms but also destroys a large variety of chemical contaminants.[17−19] This capability is very desirable for the disinfection of plant pathogenic fungi because it could also decompose mycotoxins produced by fungi at the same time. In recent years, TiO_2-based photocatalytic disinfection had also been successfully demonstrated as one of the novel approaches for the control and inactivation of plant pathogenic fungi.[9,11,20−22] However, due to the relatively wide band gap of TiO_2 (anatase ∼3.2 eV), most of these reports relied on UV light (λ < 400 nm) as the excitation light source, while UV light only accounts for ∼5% of the solar spectrum. Thus, it is necessary to develop novel photocatalytic materials that can yield high photocatalytic activity under visible light illumination so that a greater portion of the solar spectrum could be utilized.

Recently, anion-doping or/and transition metal ion modification had been demonstrated to be a promising approach to introduce visible light activity to TiO_2.[23−25] In our previous work, a highly efficient photocatalytic material system, palladium-modified nitrogen-doped titanium oxide (TiON/PdO), was developed, which demonstrated strong photocatalytic disinfection performance on various microorganisms, including virus, gram-negative bacteria, gram-positive bacteria, and bacterial spores, under visible light illumination.[26−30] In TiON/PdO, palladium modification served as the trapping center to photoelectrons, which reduced the e^-/h^+ pair recombination rate and subsequently increased the lifetime of charge carriers for much higher production of ROSs.[27,28] Thus, it has demonstrated a much stronger photocatalytic disinfection effect on common bacteria such as *Escherichia coli*, *Staphylococcus aureus*, and *Pseudomonas aeruginosa* than TiO_2 or $TiO_{2-x}N_x$.[31] The presence of these TiON/PdO nanoparticles in the aqueous environment did not affect the growth of zebrafish, suggesting that these TiON/PdO nanoparticles should not pose a hazardous threat to the environment.

On the other hand, it should be noted that plant pathogenic fungi usually have stronger resistance to ROSs attack than bacteria or viruses, because of their much larger size and thicker cell wall/membrane. Thus, effective alternatives to chemical fungicides are difficult to develop. Because of the demonstrated strong photocatalytic disinfection effect under visible light illumination and environmental friendliness of TiON/PdO nanoparticles, they might provide an efficient fungicidal effect. Here, we report the first photocatalytic disinfection study of *F. graminearum* multicellular macroconidia by TiON/PdO nanoparticles under visible light illumination. The cell vitality was further examined by a *Funga*Light CFDA, AM/Propidium Iodide Yeast Vitality Kit to confirm the disinfection effect. SEM observations were also conducted to examine the morphology of the *F. graminearum* multicellular macroconidia after their interaction with TiON/PdO nanoparticles under visible light illumination.

2. MATERIALS AND METHODS

2.1. Photocatalyst Synthesis and Characterization. TiON/PdO nanoparticles were prepared by a sol−gel method. A mixture of titanium tetraisopropoxide and tetramethylammonium hydroxide (mol ratio at 5:1) was first made in absolute ethanol. Then, a proper amount of $Pd(acac)_2$ dissolved in CH_2Cl_2 was added (Pd/Ti mol ratio at 1:200). The mixture obtained was loosely covered, and stirring was continued until a homogenous gel formed. The hydrolysis of precursors was initiated by exposure to moisture in air. The gel was aged in air for several days to allow further hydrolysis and drying. Then, the xerogel was crushed into fine powders and calcinated at 500 °C in air for 5 h to obtain the desired nanoparticle photoctalysts. The crystal structure of the nanoparticle photocatalyst was analyzed by X-ray diffraction (XRD) using a D/MAX-2004 X-ray powder diffractometer (Rigaku Corporation, Tokyo, Japan) with Ni-filtered Cu (0.15418 nm) radiation at 56 kV and 182 mA. The particle size distribution of the nanoparticle photocatalyst in distilled water was analyzed by a Particle Size Analyzer (Nano-ZS90, Malvern, UK). X-ray photoelectron spectroscopy (XPS) measurements were made using an ES CALAB250 X-ray photoelectron spectrometer (Thermo Fisher Scientific Inc., Waltham, MA) with an Al K anode (1486.6 eV photon energy, 300 W). The optical absorbance spectra of these nanoparticles were recorded in a UV-visible spectrophotometer (Jasco V-550).

2.2. Fungal Conidial Culture and Viability Assay. The *Fusarium* strain was originally obtained from wild fungi in soil cultures in Sichuan province, P. R. China. *Fusarium* colonies were inoculated into solid PDA medium, which was prepared by mixing 200 g of potato, 20 g of agar, and 1000 mL of H_2O together and then treated by autoclave. The strain was incubated in a constant temperature incubator at 26 °C for 4 days. Four pieces of *Fusarium* fungi mycelium (0.7 cm in diameter) were directly transplanted to the sporulation CMC medium, which was prepared by mixing 7.5 g of carboxymethyl cellulose ester, 0.5 g of NH_4NO_3, 0.5 g of KH_2PO_4, 0.25 g of $MgSO_4{\cdot}7H_2O$, 0.5 g of yeast extract, and 1000 mL of H_2O together and then treated by autoclave. The fungi were cultivated on a rotary shaker (KYC-100C, Shanghai CIMO Medical Instrument Manufacturing Co., LTD) under 120 rpm at 26 °C for another 4 days. Then, the mycelium was filtered by a four-layer sterile gauze, and spores were harvested from filterable CMC medium by centrifugation at 6000 rpm for 10 min at room temperature and then washing twice with distilled water. The macroconidia concentration was determined by the chamber for counting blood cells under a phase contrast microscope. The macroconidia suspension was diluted in distilled water to the concentration of ∼2×10^6 CFU/mL before its use in photocatalytic inactivation experiments. All solid or liquid materials had been autoclaved for 30 min at 121 °C before use.

A 300 W xenon lamp (PLS-SXE300, Beijing Perfect Light Technology Co. Ltd., Beijing, China) was used for photocatalytic inactivation experiments, and the light with wavelengths below 400 nm and above 700 nm was blocked by glass filters. The light intensity striking the spore suspensions was at ca. 20 mW/cm^2, as measured by a FZ-A optical Radiometer (Photoelectric Instrument Factory of Beijing Normal University, Beijing, China). In this study, a fixed concentration of 1 mg photocatalyst/mL spore suspension was used. In the photocatalytic inactivation experiment, an aliquot of 9 mL of distilled water with 10 mg TiON/PdO nanoparticles was first injected into a sterile 60 mm × 15 mm Petri dish and was dispersed ultrasonically for 10 min. Then, 1 mL of spore suspension (2×10^6 CFU/mL) was added into the Petri dish. Magnetic stirring was used, and no electron acceptor was added during the photocatalytic treatment. The experiment was conducted at room temperature (∼25 °C) with a temperature control system. At regular time intervals, 100 μL aliquots of the treated spore suspensions were withdrawn in sequence for fluorescent staining, and another 100 μL aliquot was withdrawn simultaneously for viability array experiments. The detection limitation for the plating assay with 100 μL sample solution is 10 CFU/mL. Following the appropriate dilution in PBS buffer solution (pH 7), aliquots of 100 μL were spread onto an agar medium plate. After a 48 h incubation at 26 °C in the constant temperature incubator, the number of viable cells in terms of colony-forming units was counted. The survival ratio was determined by $N(t)/N(t_0)$, where $N(t)$ was the number of colony-forming units at the treatment time t and $N(t_0)$ was the number of colony-forming units at time zero. For comparison purposes, the photocatalytic antifungal performance of Degussa P25 TiO_2 nanoparticles (Evonik Industries, Germany) was also examined with the same experiment conditions. Control runs were carried out either with no photocatalyst in the spore suspension under the same visible light illumination or with photocatalysts in the dark. All analyses were in triplicate.

2.3. Fluorescence Staining of Macroconidia. The *Funga*Light CFDA, AM/Propidium Iodide Yeast Vitality Kit (Molecular Probes,

USA) was applied to reveal the vitality of macroconidia with or without photocatalytic treatment. According to the manufacture, *Funga*Light CFDA, AM/Propidium Iodide Yeast Vitality Kit combines a cell permeable esterase substrate with a membrane integrity indicator to evaluate the vitality of macroconidia cells by fluorescence microscopy. The acetoxymethyl ester (AM) of the esterase substrate 5-car esterases diacetate (CFDA) allows this reagent to permeate cell membranes. Once inside the cell, the lipophilic blocking and diacetate groups are cleaved by nonspecific esterases, resulting in a fluorescent, charged form that leaks out of cells very slowly, while the propidium iodide, as a membrane integrity indicator, could only penetrate cell with damaged membranes. With an appropriate mixture of the CFDA, AM, and propidium iodide stains, esterase active cells with intact cell membranes stain fluorescent green, whereas cells with damaged membranes stain fluorescent red. The stain procedure followed the manuals and protocols described in the *Funga*Light Kit. The CFDA, AM, and propidium iodide were dissolved in DMSO, respectively, and then kept at −20 °C with protection from light. When needed, 1 μL of each was added into 1 mL of cell sample. Samples were then incubated in the dark at 37 °C for 30 min. After incubation, samples were washed 3 times and resuspended in a 50 μL volume of PBS. A 20 μL suspension was dropped onto a glass slide and then covered with a clear glass coverslip. A Nikon 80i upright research-grade microscope was configured to perform the fluorescence and phase contrast microscopy observation. A mercury lamp (U-LH100HG, 100W) was used as the light source, and FITC/TRITC filter was used. Images were recorded through a Color Cooled Digital Camera Head (DS-Fi1c) with the 10× and 40× objectives.

2.4. Scanning Electron Microscopy Observation. Spores without or with photocatalytic treatment were collected by centrifugation. The pellet was fixed with 2.5% glutaraldehyde and 4% paraformaldehyde in 0.1 M phosphate buffer at 4 °C for 2 h. After fixation, the cell pellets were washed with phosphate buffer for three times to remove the excess fixative. Then, the samples were dehydrated by a successive soaking in 50%, 70%, and 90% (v/v) ethanol for 10 min each and three soakings in absolute ethyl alcohol for 15 min each. The pellets were then soaked in isoamyl acetate for 1 h. Critical point drying was performed by placing samples in hexamethyl disilazane for 45 min and allowing them to dry overnight at room temperature. SEM images of the samples were obtained with a scanning electron microscope (LEO SUPRA 35, LEO, Germany) at an acceleration voltage of 20 kV. Before imaging, the samples were sputtered with gold for 120 s (Cressington Sputter Coater 208HR, Cressington Scientific Instrument Ltd., UK).

3. RESULTS AND DISCUSSION

3.1. Characterization of TiON/PdO Nanoparticles. Figure 1a shows the X-ray diffraction pattern of TiON/PdO nanoparticles, which demonstrates that only anatase phase is present and no rutile phase exists. The average crystallite size was ∼11 nm, which was calculated by the Scherrer's formula from the strongest XRD peak in Figure 1a. Besides the anatase structure, a weak diffraction peak at $2\theta \sim 34.7°$ was identified, which could be assigned to PdO (101) XRD diffraction peak. The XRD result suggested that the palladium additive existed as PdO and did not substitute titanium as the dopant in TiO_2 anatase structure. Figure 1b shows the TEM image of TiON/PdO nanoparticles. They were nanosized particles with nonuniform shapes, and the average particle size was ∼10 to 20 nm. These nanoparticles were aggregated into larger particles in distilled water, and the average aggregate size was ∼246.4 nm as determined from the particle size distribution analysis. Figure 1c shows the representative XPS survey spectrum of TiON/PdO nanoparticles, confirming the presence of Ti, Pd, O, and N in the sample. The relative element composition ratio was determined by multiplex high-resolution scans over Ti 2p, Pd 3d, O 1s, and N 1s spectral regions, and

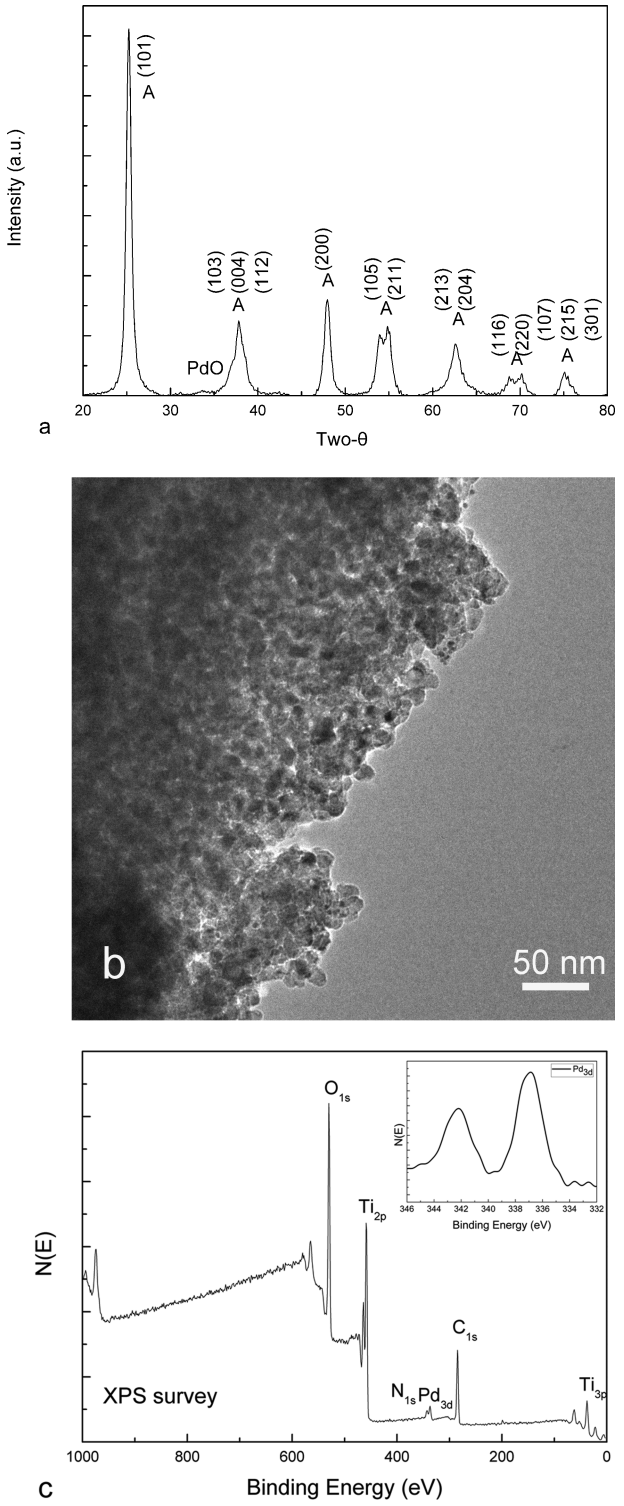

Figure 1. (a) X-ray diffraction pattern of TiON/PdO nanoparticle photocatalyst (A, anatase). (b) Transmission electron microscopy image of palladium-modified nitrogen-doped titanium oxide nanoparticle powders. (c) Representative XPS survey spectrum of TiON/PdO nanoparticles. (Note: Inset plot illustrates the high-resolution XPS scan spectrum over Pd 3d spectral region of TiON/PdO nanoparticles.)

the average atomic ratios of N/Ti and Pd/Ti were ∼0.03 and ∼0.04, respectively. The average atomic ratio of Pd/Ti was higher than its ratio in the raw material, which could be attributed to the accumulation of the palladium additive on the

dx.doi.org/10.1021/am4031196 | ACS Appl. Mater. Interfaces 2013, 5, 10953−10959

surface of TiON because it could not enter TiO_2 anatase structure. The inset plot is the high-resolution scan over Pd 3d spectral region. The binding energy of Pd 3d 5/2 was ~336.8 eV, which also suggested that Pd additive existed as PdO in these TiON/PdO nanoparticles and was in accordance with their XRD result.

The optical properties of TiON/PdO nanoparticles were investigated by measuring their diffuse reflectance spectrum. From the reflectance data, optical absorbance could be approximated by the Kubelka-Munk function, as given by the following equation:

$$F(R) = \frac{(1-R)^2}{2R} \quad (1)$$

where R is the diffuse reflectance.[32] Figure 2a shows the light absorbance (in terms of Kubelka-Munk equivalent absorbance units) of TiON/PdO nanoparticles, compared with the commercially available Degussa P25 TiO_2 powder. P25 demonstrated the characteristic light adsorption spectrum with the fundamental absorbance stopping edge at ~400 nm, which suggested that its photocatalytic activity was mainly within the UV light region. TiON/PdO nanoparticles, however, demonstrated a strong visible light absorbance from 400 to 700 nm. The visible light absorbance capability of TiON/PdO nanoparticles could be attributed to both the nitrogen-doping effect[23] and the transition metal modification enhancement from SPR effect.[33] Figure 2b shows the Tauc plot ($(F(R) \times h\nu)^n$ vs $h\nu$) constructed from Figure 2a, which shows the linear Tauc region just above the optical absorption edge to determine the semiconductor band gap. For a direct band gap semiconductor, n equals 0.5. Extrapolation of this line to the photon energy axis yields the semiconductor band gap. The band gap of the Degussa P25 TiO_2 nanoparticles was determined at ~3.24 eV, which agrees with other reports.[23,34] TiON/PdO nanoparticles, however, demonstrated a much smaller band gap of ~1.71 eV, which agreed well with their good visible light absorbance.

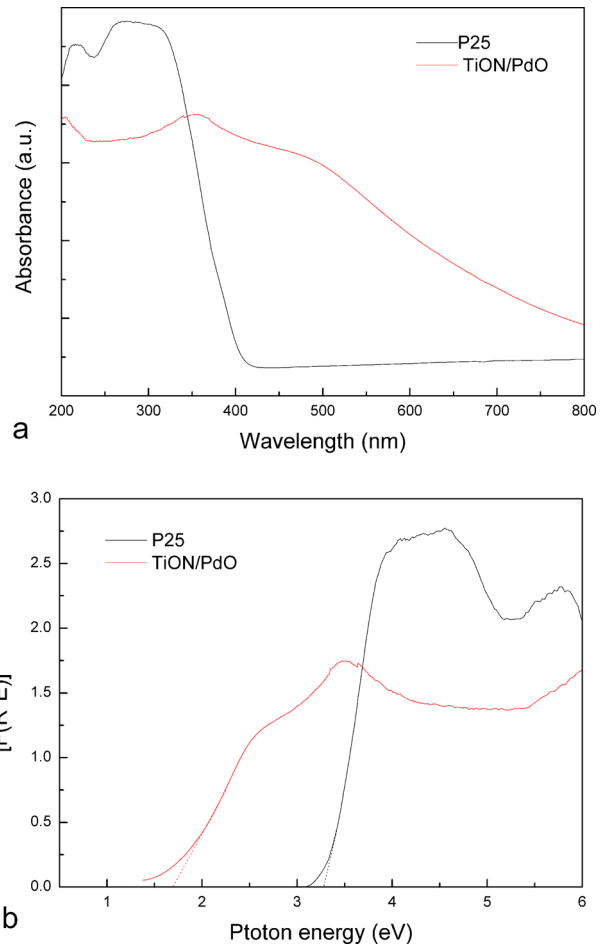

Figure 2. (a) Optical absorbance (in terms of Kubelka-Munk equivalent absorbance units) of TiON/PdO nanoparticles, compared with that of P25 TiO_2 nanoparticles. (b) Tauc Plot of TiON/PdO and P25 TiO_2 nanoparticles constructed from (a).

3.2. Photocatalytic Disinfection of *Fusarium Graminearum* Macroconidia under Visible Light Illumination.

Figure 3 demonstrates the survival ratio of the wild type *F. graminearum* macroconidia treated by TiON/PdO nanoparticles under visible light illumination (λ > 400 nm), compared with that of the wild type *F. graminearum* macroconidia treated by visible light illumination only (control), treated by Degussa P25 TiO_2 nanoparticles under visible light illumination, and treated by TiON/PdO nanoparticles in the dark, respectively. With only visible light illumination, no obvious loss of the survival ratio of the wild type *F. graminearum* macroconidia was observed. Degussa P25 TiO_2 nanoparticles were widely used as model TiO_2 nanoparticles for the photocatalytic microorganism disinfection research. For example, Sichel et al.[9] reported in 2007 that Degussa P25 TiO_2 nanoparticles had efficient disinfection effect on a well-known soilborne pathogen, *Fusarium. solani* conidia. Its concentration could be reduced from 10^3 to10^1 CFU/mL within 2 h under the solar irradiation. However, no obvious loss of the survival ratio of the wild type *F. graminearum* macroconidia was observed by its treatment, although Degussa P25 TiO_2 nanoparticles could possess the photocatalytic

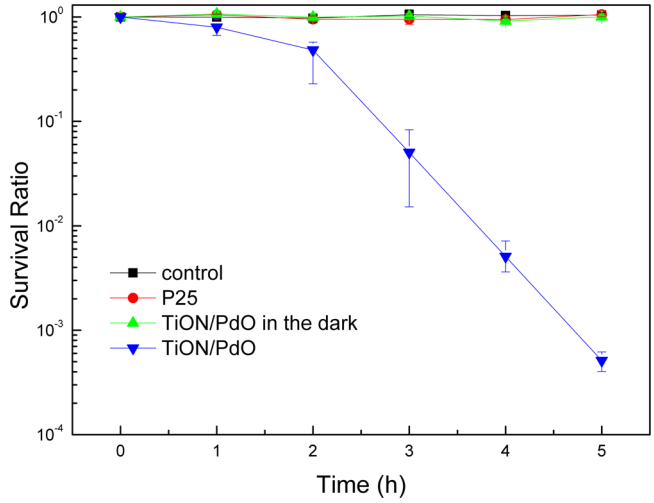

Figure 3. Survival ratio of *F. graminearum* macroconidia versus various treatments: under visible light illumination without photocatalyst (black squares), under visible light illumination (400−700 nm) with P25 nanoparticles (red circles), in the dark with TiON/PdO nanoparticles (green triangles), and under visible light illumination with TiON/PdO nanoparticles (inverted, blue triangles). The macroconidia suspension had an initial concentration at ca.10^5 CFU/mL. The data shown were the average values from three experiments.

activity under visible light illumination due to its mixture nature of rutile and anatase TiO_2 phases.[35] After 5 h of visible light illumination, the survival ratio of the wild type *F. graminearum* macroconidia was still ~100%, indicating that its photocatalytic disinfection capability could not disinfect the wild type *F. graminearum* macroconidia under visible light illumination.

TiON/PdO nanoparticles, however, demonstrated a superior photocatalytic disinfection capability on the wild type *F. graminearum* macroconidia under visible light illumination. Without visible light illumination, the survival ratio of the wild type *F. graminearum* macroconidia was kept at ~100% after 5 h treatment with TiON/PdO nanoparticles, indicating that TiON/PdO nanoparticles were not toxic to *F. graminearum* macroconidia by themselves. With visible light illumination, a sharp decrease of the survival ratio of the wild type *F. graminearum* macroconidia was observed when TiON/PdO nanoparticles were present. Their survival ratio dropped relatively slowly to ~79% and ~48% at 1 and 2 h after the beginning of the photocatalytic treatment, respectively, and then dropped sharply. Their survival ratio decreased to $\sim 5.12 \times 10^{-4}$ after 5 h treatment, which was more than three orders of magnitude lower, compared with that treated by Degussa P25 TiO_2 nanoparticles. Such a strong photocatalytic disinfection effect on *F. graminearum* macroconidia had not been reported in literature. Compared with the commonly used model microorganism *E. coli* bacteria,[28,29,36] it is clear that the resistance of these *F. graminearum* macroconidia to the photocatalytic disinfection is stronger, which could be attributed to their different cell sizes and structures.[37] The *F. graminearum* macroconidium usually has 4 to 6 cells, and its size is about 25−70 μm × 3−5 μm, which is much larger than that of *E. coli* bacteria. The membrane/cell wall of *F. graminearum* macroconidia is also much thicker than that of *E. coli* bacteria. Thus, their resistance to the attack from ROSs is stronger,[37] and a more powerful photocatalyst than Degussa P25 TiO_2 nanoparticles is needed for their effective disinfection. For TiON/PdO nanoparticles, the effective electron−hole pair separation from the electron trapping on PdO nanoparticles[28,29] could largely increase the lifetime of highly reactive holes for more efficient production of highly active ·OH radicals for their demonstrated largely enhanced photocatalytic disinfection efficiency on *F. graminearum* macroconidia.

3.3. Photocatalytic Disinfection Mechanism Study of *Fusarium Graminearum* Macroconidia by Fluorescent/Phase Contrast Microscopy. The vital dye staining technique was widely used to examine the cell activity in photocatalytic disinfection studies.[36,38−40] The photocatalytic disinfection of *F. graminearum* macroconidia was further examined by the fluorescent observation of these macroconidia after being stained with the *Funga*Light CFDA, AM/Propidium Iodide Yeast Vitality Kit to reveal their vitality after different treatments. Figure 4a demonstrates that most of the macroconidia in the sample were stained green by the *Funga*Light CFDA, AM/Propidium Iodide Yeast Vitality Kit when they were only illuminated by the visible light illumination for 5 h without the presence of TiON/PdO nanoparticles. This observation indicated that they were viable and had intact membranes, further verifying that the visible light illumination only could not be toxic to them. Figure 4b demonstrates that most of the macroconidia in the sample were stained green when they were treated in the dark for 5 h with the presence of TiON/PdO nanoparticles. This observation indicated that they were viable and had intact membranes, further verifying that TiON/PdO nanoparticles could not be toxic to them without the visible light illumination. When both the visible light illumination was on and TiON/PdO nanoparticles were present, more and more *F. graminearum* macroconidia were stained red with the illumination time increase from 1 h (Figure 4c) to 3 h (Figure 4d) to 5 h (Figure 4e) by the probe of propidium iodide. After a 5 h photocatalytic treatment, almost all the cells were stained red, which was in accordance with the plating assay results demonstrated in Figure 3. Because propidium iodide could only penetrate cells with damaged membranes to stain these cells red, the observation of the increase of red cells during the photocatalytic treatment indicated that more and more *F. graminearum* macroconidia were damaged with the photocatalytic treatment, which allowed propidium iodide to penetrate into the cells and also led to the leakage of cell contents from the damaged membranes. In Figure 4c,d, it was observed that one macroconidium could have sections with different stained colors.

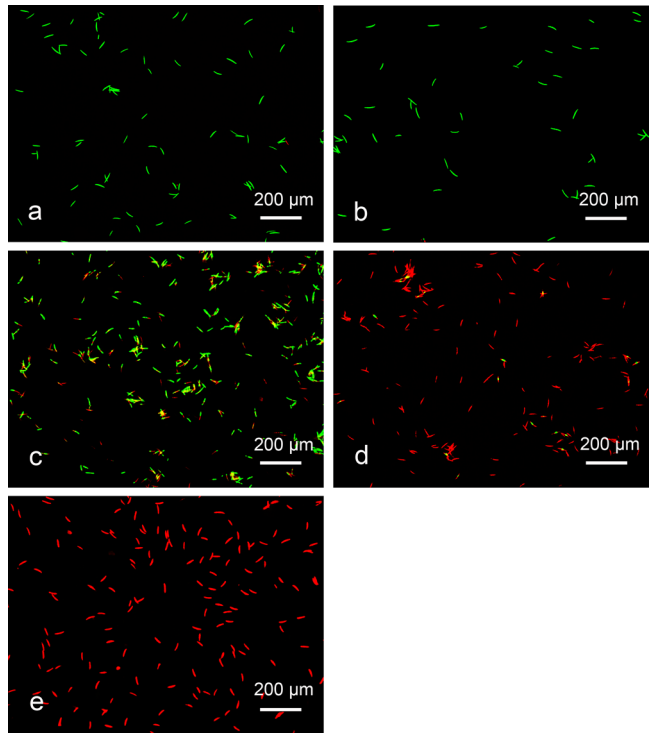

Figure 4. *F. graminearum* macroconidia viability as detected by CFDA, AM/Propidium Iodide. The live cell appears green while the dead ones are red: (a) after illumination for 5 h without photocatalyst; (b) in the dark after 5 h with photocatalyst; (c) after photocatalytic treatment for 1 h; (d) after photocatalytic treatment for 3 h; (e) after photocatalytic treatment for 5 h.

To further examine the apparent morphology changes of *F. graminearum* macroconidia with or without the presence of TiON/PdO nanoparticles under visible light illumination, the phase contrast microscopic observation was used to supplement the fluorescent observation. Figure 5a,b demonstrates the enlarged fluorescent observation of *F. graminearum* macroconidia in Figure 4a,c, respectively, and their corresponding phase contrast images were shown in Figure 5c,d. Figure 5e,f shows the phase contrast images of one macroconidium in Figure 5c,d, respectively, with a higher magnification. Unlike the simple single-cell *E. coli* bacteria, the macroconidium of *F. graminearum* is a eukaryotic multicellular organism, which

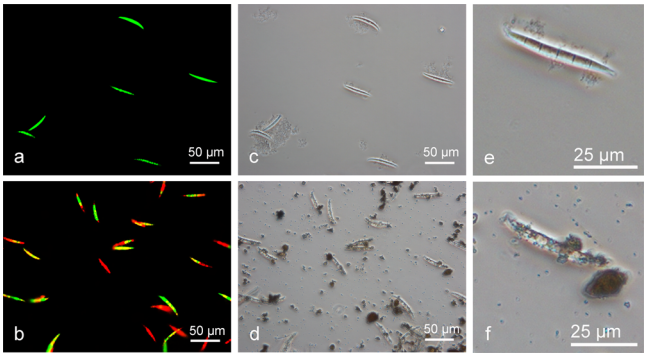

Figure 5. Fluorescent images (a and b) and the corresponding phase contrast microscope images (c and d) showing membrane damage and cell viability of the *F. graminearum* macroconidia without or with photocatalyst: (a/c) after illumination for 5 h without photocatalyst; (b/d) after photocatalytic treatment for 1 h; (e/f) is the enlarged observation of macroconidia in (c/d).

typically has 4 to 6 cells demarcated by septa.[37] The two apical cells of the slender, elongated macroconidium possess obvious asymmetry, and each one gradually tapers toward a rounded end (see Figure 5c). Figure 5a demonstrated that these *F. graminearum* macroconidia had excellent viability with bright stained green color after being illuminated with visible light for 5 h without the presence of TiON/PdO nanoparticles. Their cell structures were complete in these *F. graminearum* macroconidia in the corresponding phase contrast images (Figure 5c,e).

After being treated with TiON/PdO nanoparticles for 1 h under visible light illumination, some macroconidia still had viability with stained green color, while some macroconidia lost their viability as demonstrated by their stained red color (see Figure 5b). Interestingly, some macroconidia were stained with yellow color (see Figure 5b), which should come from the combination of the green stain by CFDA and AM and the red stain by propidium iodide at the same time. Thus, those cells should have damaged cell membrane to allow propidium iodide to enter them, but they still kept part of their viability so they could also be stained by CFDA and AM at the same time. The damages caused by ROSs attacks may occur on any cell in one macroconidium demarcated by septa. Thus, different cells in this macroconidium may have different colors. That is why green, red, and even yellow color could be observed in one macroconidium. The fluorescent observation (Figure 5b) and the corresponding phase contrast image (Figure 5d) also suggest that these macroconidia still kept their structure even after they lost their viability. Thus, damages on the cell membranes of the dead macroconidia were not severe enough to break their structures. The viability loss could be attributed to the leakage of the cell contents and possible entrance of ROSs into the cells after the cell membrane damage. From these observations, it could be concluded that the cell membrane damage caused by the photocatalytic process is the critical step in the disinfection of *F. graminearum* macroconidia, while the complete destruction of the cell structure to have a biocidal effect is not a prerequisite for their disinfection.

3.4. TiON/PdO Nanoparticle Attachment on *F. Graminearum* Macroconidia. In Figure 5d,f, it could be observed that the *F. graminearum* macroconidium surface was not clean and powders existed on their surface. SEM was then further used for the observation of the *F. graminearum* macroconidium morphology after various treatments. Figure 6a showed the SEM image of these macroconidia after being

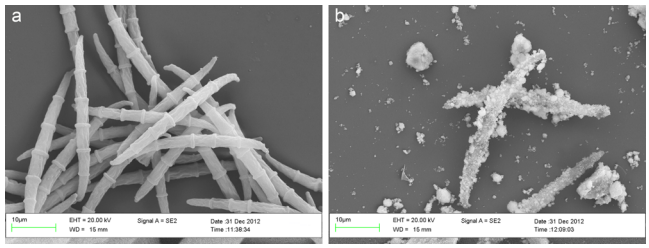

Figure 6. SEM images of *F. graminearum* macroconidia: (a) after being illuminated for 5 h without photocatalyst; (b) after photocatalytic inactivation treatment for 5 h.

illuminated by visible light for 5 h without the presence of TiON/PdO nanoparticles. In this control experiment sample, these macroconidia had the clear crinoid structure and smooth surface. Figure 6b showed the SEM image of these macroconidia after being illuminated by visible light for 5 h with the presence of TiON/PdO nanoparticles, which clearly demonstrated that TiON/PdO nanoparticles were adsorbed onto the surface of these macroconidia. The potential of zero charge (PZC) of TiON/PdO nanoparticles was determined at ~pH 3.3; thus, they were negatively charged when dispersed in the distilled water (pH ~ 6.5). In the previous work of Smither-Kopperl et al.,[41] similar *Fusarium culmorum* spores were determined to carry positive charges as they migrated towards the negative pole during electrophoresis in both Tris-borate buffer (pH 8.3) and sodium phosphate buffer (pH 7.0). Thus, *F. graminearum macroconidia* should be positively charged in the distilled water. The attachment of TiON/PdO nanoparticles could be attributed to the opposite surface charges between TiON/PdO nanoparticles and these macroconidia. Due to the short lifetimes of both photon-excited electron-hole pairs and subsequently produced ROSs such as ·OH, $O_2^{\bullet-}$, and $HO_2^{\bullet}$, the photocatalytic reactions occur only at/near the photocatalyst surface. Thus, the attachment of TiON/PdO nanoparticles onto the surface of these macroconidia is beneficial to its photocatalytic disinfection effect on these macroconidia.[42]

4. CONCLUSION

In summary, TiON/PdO nanoparticles synthesized by a sol–gel process demonstrated a good visible light adsorption and a superior efficient photocatalytic disinfection effect on *F. graminearum* macroconidia under visible light illumination. Within hours of light illumination, TiON/PdO nanoparticles reduced the survival ratio of the *F. graminearum* macroconidia by more than three orders of magnitude. The disinfection effect benefitted from the adsorption of TiON/PdO nanoparticles onto the *F. graminearum* macroconidia surface due to their opposite surface charges. The fluorescence/phase contrast microscopy observations demonstrated that the photocatalytic disinfection mechanism of TiON/PdO nanoparticles on these macroconidia could be attributed to their cell wall/membrane damage caused by the attack from ROSs, while the complete destruction of the cell structure to have a biocidal effect is not required. Thus, TiON/PdO photocatalyst has a great potential as an environmentally-friendly alternative method to disinfect plant pathogens for agricultural areas.

AUTHOR INFORMATION

Corresponding Author

*E-mail: qili@imr.ac.cn. Tel.: +86-24-83978028. Fax: +86-24-23971215.

Notes

The authors declare no competing financial interest.

ACKNOWLEDGMENTS

The experimental assistance for the *F. graminearum* culture by Ms. Mian Song and Ms. Shuang Jiao was greatly appreciated. This study was supported by the National Natural Science Foundation of China (Grant No. 51102246), the Knowledge Innovation Program of Institute of Metal Research, Chinese Academy of Sciences (Grant No. Y0N5A111A1), the Youth Innovation Promotion Association, Chinese Academy of Sciences (Grant No. Y2N5711171), and the Scientific Research Foundation for the Returned Overseas Chinese Scholars, State Education Ministry, China.

REFERENCES

(1) Parry, D. W.; Jenkinson, P.; McLeod, L. *Plant Pathol.* **1995**, *44*, 207−238.
(2) McMullen, M.; Jones, R.; Gallenberg, D. *Plant Dis.* **1997**, *81*, 1340−1348.
(3) Harris, S. D. *Mycologia* **2005**, *97*, 880−887.
(4) Elad, Y.; Yunis, H.; Katan, T. *Plant Pathol.* **1992**, *41*, 41−46.
(5) Matsunaga, T.; Tomoda, R.; Nakajima, T.; Wake, H. *FEMS Microbiol. Lett.* **1985**, *29*, 211−214.
(6) Sjogren, J. C.; Sierka, R. A. *Appl. Environ. Microbiol.* **1994**, *60*, 344−347.
(7) Kangwansupamonkon, W.; Lauruengtana, V.; Surassmo, S.; Ruktanonchai, U. *Nanomedicine* **2009**, *5*, 240−249.
(8) Xing, Y.; Li, X.; Zhang, L.; Xu, Q.; Che, Z.; Li, W.; Bai, Y.; Li, K. *Prog. Org. Coat.* **2012**, *73*, 219−224.
(9) Sichel, C.; de Cara, M.; Tello, J.; Blanco, J.; Fernández-Ibáñez, P. *Appl. Catal., B* **2007**, *74*, 152−160.
(10) Yao, K. S.; Wang, D. Y.; Ho, W. Y.; Yan, J. J.; Tzeng, K. C. *Surf. Coat. Technol.* **2007**, *201*, 6886−6888.
(11) Wolfrum, E. J.; Huang, J.; Blake, D. M.; Maness, P.-C.; Huang, Z.; Fiest, J.; Jacoby, W. A. *Environ. Sci. Technol.* **2002**, *36*, 3412−3419.
(12) Rodríguez-González, V.; Alfaro, S. O.; Torres-Martínez, L. M.; Cho, S.-H.; Lee, S.-W. *Appl. Catal., B* **2010**, *98*, 229−234.
(13) Sökmen, M.; Değerli, S.; Aslan, A. *Exp. Parasitol.* **2008**, *119*, 44−48.
(14) Maneerat, C.; Hayata, Y. *Int. J. Food Microbiol.* **2006**, *107*, 99−103.
(15) Chawengkijwanich, C.; Hayata, Y. *Int. J. Food Microbiol.* **2008**, *123*, 288−292.
(16) Bodaghi, H.; Mostofi, Y.; Oromiehie, A.; Zamani, Z.; Ghanbarzadeh, B.; Costa, C.; Conte, A.; Del Nobile, M. A. *LWT - Food. Sci. Technol.* **2013**, *50*, 702−706.
(17) Li, Q.; Mahendra, S.; Lyon, D. Y.; Brunet, L.; Liga, M. V.; Li, D.; Alvarez, P. J. *Water. Res.* **2008**, *42*, 4591−4602.
(18) Konaka, R.; Kasahara, E.; Dunlap, W. C.; Yamamoto, Y.; Chien, K. C.; Inoue, M. *Free Radical Biol. Med.* **1999**, *27*, 294−300.
(19) Wist, J.; Sanabria, J.; Dierolf, C.; Torres, W.; Pulgarin, C. *J. Photochem. Photobiol., A* **2002**, *147*, 241−246.
(20) Lonnen, J.; Kilvington, S.; Kehoe, S. C.; Al-Touati, F.; McGuigan, K. G. *Water Res.* **2005**, *39*, 877−883.
(21) Maneerat, C.; Hayata, Y. *Int. J. Food Microbiol.* **2006**, *107*, 99−103.
(22) Hebeish, A. A.; Abdelhady, M. M.; Youssef, A. M. *Carbohydr. Polym.* **2013**, *91*, 549−559.
(23) Asahi, R.; Morikawa, T.; Ohwaki, T.; Aoki, K.; Taga, Y. *Science* **2001**, *293*, 269−271.
(24) Shah, S. I.; Li, W.; Huang, C.-P.; Jung, O.; Ni, C. *Proc. Natl. Acad. Sci. U.S.A.* **2002**, *99*, 6482−6486.
(25) Li, Q.; Xie, R.; Mintz, E. A.; Shang, J. K. *J. Am. Ceram. Soc.* **2007**, *90*, 1045−1050.
(26) Li, Q.; Xie, R.; Mintz, E. A.; Shang, J. K. *J. Am. Ceram. Soc.* **2007**, *90*, 3863−3868.
(27) Li, Q.; Page, M. A.; Mariñas, B. J.; Shang, J. K. *Environ. Sci. Technol.* **2008**, *42*, 6148−6153.
(28) Li, Q.; Li, Y. W.; Wu, P.; Xie, R.; Shang, J. K. *Adv. Mater.* **2008**, *20*, 3717−3723.
(29) Li, Q.; Li, Y. W.; Liu, Z.; Xie, R.; Shang, J. K. *J. Mater. Chem.* **2010**, *20*, 1068−1072.
(30) Wu, P.; Xie, R.; Shang, J. K. *J. Am. Ceram. Soc.* **2008**, *91*, 2957−2962.
(31) Wu, P.; Xie, R.; Imlay, J. A.; Shang, J. K. *Appl. Catal., B* **2009**, *88*, 576−581.
(32) Tauc, J.; Grigorovici, R.; Vancu, A. *Phys. Status Solidi B* **1966**, *15*, 627−637.
(33) Li, Q.; Liang, W.; Shang, J. K. *Appl. Phys. Lett.* **2007**, *90*, 063109.
(34) Tatsuma, T.; Takeda, S.; Saitoh, S.; Ohko, Y.; Fujishima, A. *Electrochem. Commun.* **2003**, *5*, 793−796.
(35) Shi, W.; Yang, W.; Li, Q.; Gao, S.; Shang, P.; Shang, J. *Nanoscale Res. Lett.* **2012**, *7*, 1−9.
(36) Wu, P.; Imlay, J. A.; Shang, J. K. *Biomaterials* **2010**, *31*, 7526−7533.
(37) Seong, K.-Y.; Zhao, X.; Xu, J.-R.; Güldener, U.; Kistler, H. C. *Fungal Genet. Biol.* **2008**, *45*, 389−399.
(38) Zhang, L.-S.; Wong, K.-H.; Yip, H.-Y.; Hu, C.; Yu, J. C.; Chan, C.-Y.; Wong, P.-K. *Environ. Sci. Technol.* **2010**, *44*, 1392−1398.
(39) Pigeot-Rémy, S.; Simonet, F.; Atlan, D.; Lazzaroni, J.; Guillard, C. *Water Res.* **2012**, *46*, 3208−3218.
(40) Thabet, S.; Weiss-Gayet, M.; Dappozze, F.; Cotton, P.; Guillard, C. *Appl. Catal., B* **2013**, *140-141*, 169−178.
(41) Smither-Kopperl, M. L.; Charudattan, R.; Berger, R. D. *Phytopathology* **1998**, *88*, 382−388.
(42) Herrmann, J. M. *Top. Catal.* **2005**, *34*, 49−65.